

Review

Evolution of Fiber-Optic Transmission and Networking toward the 5G Era

Xiang Liu^{1,*}

OPENING REMARKS

Optical networks are supporting a wide range of communication services including residential services, enterprise services, and mobile services. Figure 1 illustrates a typical end-to-end optical communication network consisting of core, metro, and access optical networks. The upcoming fifth-generation (5G) wireless network brings to optical networking new requirements such as high bandwidth, low latency, accurate synchronization, and the ability to perform network slicing. The requirement for high bandwidth is driven by emerging wireless applications such as massive multiple-input-multiple-output (MIMO), whereas the requirements for low latency and accurate synchronization are mainly driven by applications such as cloud radio access network (C-RAN) and coordinated multi-point (CoMP). The requirement for network slicing is aimed at optimizing the resource utilization for any given application. All these requirements are to be addressed in the so-called 5G-oriented optical networks. This review aims to highlight the dramatic technological advances in fiber-optic transmission and networking over the last few years and provide perspectives on what to expect in the coming era of 5G. The content of this review is outlined as follows:

- Historical aspects—overview of fiber-optic transmission and networking
- Enhanced fiber transmission capacity (eFTC)
 - Optical modulation and detection technologies
 - Superchannel transmission
 - Exploring the capacity limit in optical fiber transmission
- Reconfigurable optical add/drop multiplexer (ROADM) and optical cross-connect (OXC)
- Ultra-broadband optical access
- 5G-oriented optical transport networks
- Intelligent network operation and maintenance (iO&M)
- Conclusion and outlook

HISTORICAL ASPECTS—OVERVIEW OF FIBER-OPTIC TRANSMISSION AND NETWORKING

Fiber-optical communications benefited from many groundbreaking scientific advances in the field of optics, photonics, electronics, and digital signal processing (DSP) (Agrell et al., 2016; Kaminow et al., 2013; Winzer et al., 2018). The following list highlights some of the relevant breakthroughs and events (Hecht, 2004):

1880: Alexander Graham Bell invented Photophone

1948: Claude Shannon formulated the Shannon Limit of a communication channel (Shannon, 1948)

1957: Charles Townes and Arthur Schawlow outlined principles of laser operation (Schawlow and Townes, 1958)

1966: Charles Kao concluded that the fundamental limit on glass transparency is below 20 decibels per kilometer, which would be practical for communications. Hockham calculated that clad fibers should not radiate much light. They prepared a paper proposing fiber-optic communications (Kao and Hockham, 1966)

¹New Jersey Research Center, Futurewei Technologies, Bridgewater, NJ 08807, USA

*Correspondence:

xiang.liu@futurewei.com

<https://doi.org/10.1016/j.isci.2019.11.026>



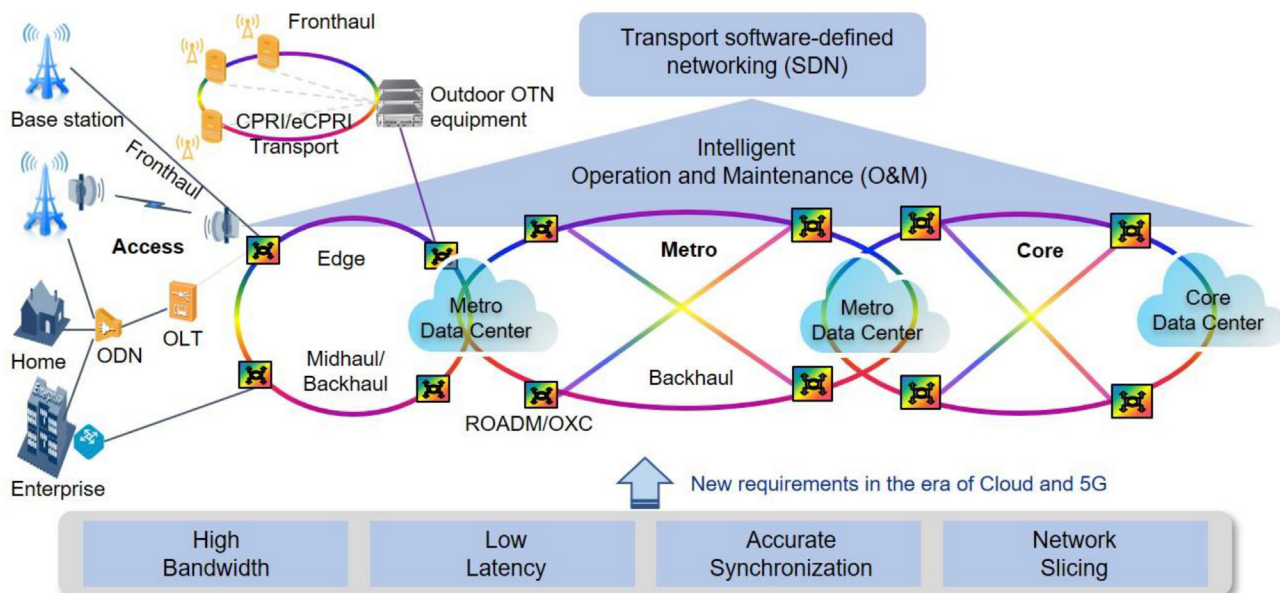


Figure 1. Illustration of a 5G-Oriented Optical Network Consisting of Core, Metro, and Access Network Sections to Support Diverse Applications
 OTN, optical transport network; CPRI, common public radio interface; eCPRI, evolved CPRI; ROADM, reconfigurable optical add/drop multiplexer; OXC, optical cross-connect; OLT, optical line terminal; ODN, optical distribution network.

1970: First continuous-wave room-temperature semiconductor lasers made in early May by Zhores Alferov's group at the Ioffe Physical Institute in Leningrad (now St. Petersburg) and on June 1 by Mort Panish and Izuo Hayashi at Bell Labs

1987: David Payne's group reported making the first erbium-doped optical fiber amplifier at the University of Southampton. Emmanuel Desurvire and Randy Giles developed a model to predict the behavior of erbium optical amplifier at Bell Labs (Mears et al., 1987; Giles and Desurvire, 1991)

1988: Linn Mollenauer of Bell Labs demonstrated soliton transmission through 4,000 km of single-mode fiber

1993: Andrew Chraplyyy et al. at Bell Labs transmitted at 10 Gb/s on each of eight wavelengths through 280 km of dispersion-managed fiber (Chraplyyy et al., 1993)

1996: Commercial wavelength-division multiplexing (WDM) systems were introduced

2002: Differential phase-shift keying (DPSK) was first demonstrated for 40 Gb/s long-haul (4,000 km) transmission by Bell Labs (Xu et al., 2004; Gnauck et al., 2002)

2002: Nonlinearity compensation in fiber transmission was introduced for phase-modulated signals by Bell Labs (Liu et al., 2002)

2003: Gigabit-capable Passive Optical Networks (G-PON) was standardized by the Telecommunication Standardization Sector of the International Telecommunication Union (ITU-T)

2004: DSP-based coherent optical detection concept was introduced by Michael Taylor of University College London (Taylor, 2004)

2009: Superchannel concept was introduced and experimentally demonstrated at 1.2 Tb/s by Bell Labs (Chandrasekhar et al., 2009)

2010: René Essiambre et al. at Bell Labs studied the Shannon Limit for nonlinear fiber-optical transmission (Essiambre et al., 2010)

2010: 10-Gigabit-capable Passive Optical Networks (XG-PON) were standardized by ITU-T

2011: Peter Winzer et al. at Bell Labs researched spatial multiplexing for optical transport capacity scaling (Winzer, 2011)

Year:	1980	1990	2000	2010	2020
Channel rate	2.5 Gb/s	10 Gb/s	40 Gb/s	100 Gb/s	200/400 Gb/s
Modulation format (typical)	OOK (NRZ)	OOK (RZ)	DPSK DQPSK	PDM-QPSK	PDM-nQAM, CS, PAM4, DMT
System features (newly added)	Single-span, Single-channel	Multi-span with EDFAs, WDM	DWDM, Raman, ROADMs	1:N WSS, CDC-ROADMs	Flexible-grid WDM, M:N WSS, Super-C EDFA
System capacity (typical)	2.5 Gb/s (single channel)	400 Gb/s (40 WDM channel)	1.6 Tb/s (40 WDM channel)	8 Tb/s (80 DWDM channel)	16~32 Tb/s (Fixed-grid or flex-grid channels)
System reach (typical)	100 km (single span)	1000 km	1000 km @40G 3000 km @10G	4000 km @100G	2000(1000) km @200(400)G
Enabling technologies	Directly modulated laser	High-speed modulation, HD-FEC	Differential phase-shift keying	Coherent detection with oDSP, SD-FEC	100Gbaud-class OE device and advanced oDSP

Table 1. Key Technologic Advances in Fiber-Optical Transmission over the Last 30 Years

2012: Flexible-grid WDM was standardized by ITU-T ([Recommendation ITU-T G.694.1, 2012](#))

2016: Low-loss low-nonlinearity optical fibers were specified by ITU-T ([Zong et al., 2016](#))

2018: Low-loss M×N colorless-directionless-contentionless (CDC) wavelength-selective switch (WSS) was developed by Lumentum ([Colbourne et al., 2018](#))

2019: Super-C-band transmission with 6-THz optical bandwidth was demonstrated by Huawei Technologies ([Huawei's ON2.0, 2019](#))

Over the past 30 years, optical fiber transmission systems have been advanced rapidly ([Agrell et al., 2016](#); [Kaminow et al., 2013](#); [Winzer et al., 2018](#)). As shown in [Table 1](#), the typical single-channel data rate of fiber-optic transmission has increased from 2.5 Gb/s in around 1989 to 400 Gb/s in 2019, which is over 100 times. The main technologies include high-speed electro-optical modulation, high-speed optical detection, hard-decision forward error correction (HD-FEC), differential binary phase-shift keying (DPSK) and quadrature phase-shift keying (DQPSK) ([Ho, 2005](#); [Winzer and Essiambre, 2006](#)), coherent optical detection assisted by digital signal processing (oDSP) ([Noe, 2005](#); [Ly-Gagnon et al., 2006](#); [Leven et al., 2006](#); [Savory, 2008](#); [Sun et al., 2008](#)), soft-decision FEC (SD-FEC), polarization-division multiplexing (PDM), high-order quadrature amplitude modulation (QAM), constellation shaping (CS) such as probabilistic CS (PCS), advanced oDSP such as faster-than-Nyquist (FTN) detection, and 100 Gbaud-class high-speed opto-electronic (OE) devices. With the introduction of super-channel technology, the aggregated channel rate can exceed 1 Tb/s ([Liu et al., 2014](#); [Chandrasekhar et al., 2009](#); [Zhou et al., 2016](#)).

In addition to an increase in data rate per channel, the number of channels per fiber is also increased through wavelength-division-multiplexing (WDM) or dense WDM (DWDM) to further improve overall transmission capacity. Besides the demand for high capacity, optical transport networks desire long unregenerated optical transmission distance to effectively support metropolitan, regional, and national network applications. The advent of fiber-optic amplifiers, such as broadband erbium-doped fiber amplifiers (EDFAs) and Raman amplifiers, has made cost-effective optical amplification of multiple WDM channels simultaneously a reality. Moreover, flexible wavelength management, enabled by elements such as reconfigurable optical add/drop multiplexers (ROADM), is often utilized to make optical networks transparent and flexible. With these advances, fiber-optic transmission system has also evolved from the initial single-span single-wavelength transmission system to today's optically amplified multi-span WDM system with reconfigurable optical add/drop sites and flexible channel grids. The typical single-fiber transmission capacity has increased significantly from 2.5 Gb/s in 1989 to 32 Tb/s in 2019, or over 10,000 times. The average single-fiber transmission capacity increase over the last 30 years is thus at a remarkable rate of over 30% per year.

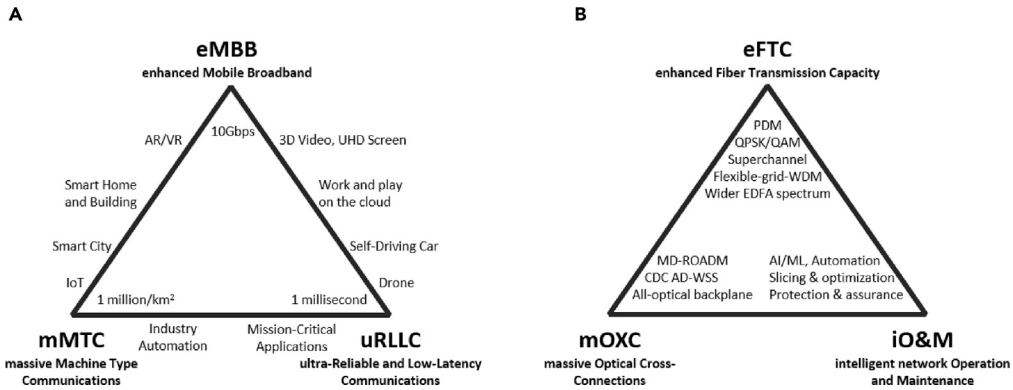


Figure 2. Main Features of 5G and 5G-oriented Fiber Optical Systems

(A) Illustration of the main features and use cases of 5G.

(B) The main features and technologies of fiber-optic networks in the 5G era. AR, augmented reality; VR, virtual reality; IoT, internet of things; UHD, ultra-high-definition; PDM, polarization-division multiplexing; QPSK, quadrature-phase-shift keying; nQAM, n-point quadrature-amplitude modulation; EDFA, Erbium-doped fiber amplifier; MD-ROADM, multi-degree reconfigurable optical add/drop multiplexer; CDC, colorless-directionless-contentionless; WSS: wavelength-selective switch; AI, artificial intelligence; ML, machine learning.

Fiber-optic transmission systems and networks are expected to continue to evolve to offer higher capacity and wider application space, especially through interworking with wireless networks. Remarkably, wireless communication has also experienced dramatic advances over the last 30 years. The first generation (1G), second generation (2G), third generation (3G), and fourth generation (4G) wireless technologies were approximately used in the decades of the 1980s, 1990s, 2000s, and 2010s, respectively (Liu, 2019). They have made significant impact on our society by providing important communication means such as mobile voice communication, text messaging, mobile internet communication, and smart phone communications. The fifth-generation wireless technology (5G) is expected to be globally launched in 2020 to provide unprecedented mobile communication experience. For 5G, there is a well-known triangle diagram to illustrate its three main features,

- enhanced mobile broadband (eMBB),
- massive machine type communications (mMTC), and
- ultra-reliable and low-latency communications (uRLLC),

as shown in Figure 2A. The three main features collectively support a vastly expanded range of service types and are forward-compatible to new services that are expected to emerge in the 5G era.

Similarly, we can use a triangle diagram to illustrate three main features of future optical networks in the decade of 2020s,

- enhanced fiber transmission capacity (eFTC),
- massive optical cross-connections (mOXC), and
- intelligent network operation and maintenance (iO&M),

as shown in Figure 2B. In the following sections, we will review key fiber-optic transmission and networking technologies in optical transceivers, optical fibers, optical amplifiers, optical cross-connects, and network controllers to collectively support the aforementioned eFTC, mOXC, and iO&M features in fiber-optic networks in the upcoming 5G era.

ENHANCED FIBER TRANSMISSION CAPACITY

To meet the demands of eMBB in 5G, optical networks need to provide more transmission capacity and do so cost-effectively. This calls for enhanced fiber transmission capacity (eFTC). The key is to increase

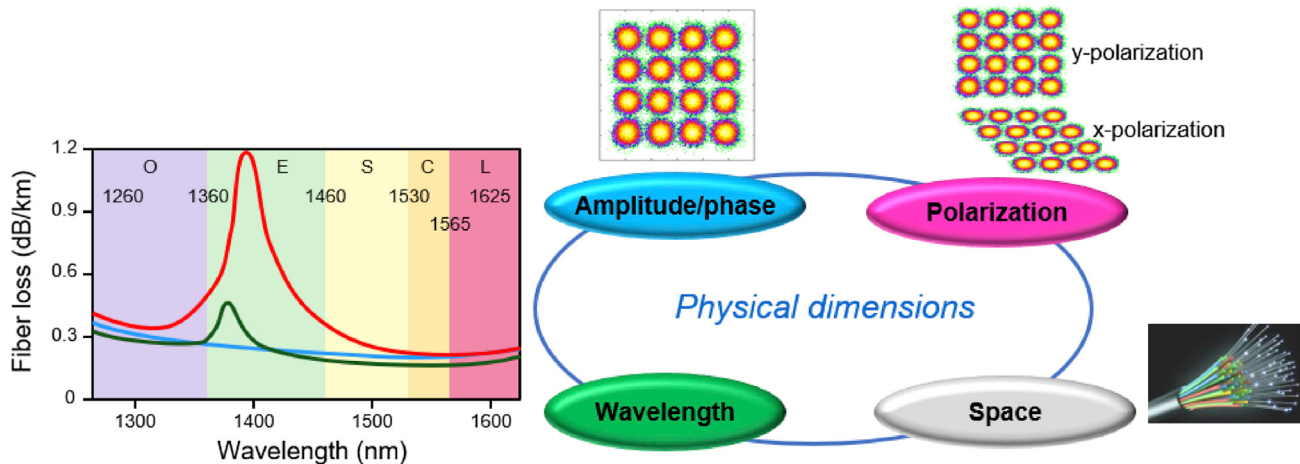


Figure 3. Illustration of Four Main Physical Dimensions that Have Been Utilized to Achieve Enhanced Fiber Transmission Capacity (eFTC)

per-fiber capacity, which can be realized by fully utilizing the following four physical dimensions of a light wave traveling along a fiber transmission link, as shown in Figure 3:

- Amplitude and phase of a given optical carrier, e.g., via quadrature-amplitude modulation and coherent detection,
- Polarization-division multiplexing (PDM), e.g., via dual-polarization modulation and detection,
- Wavelength-division multiplexing (WDM), e.g., over a broad optical amplification window, and
- Space-division multiplexing (SDM), e.g., by using multiple single-mode fibers in a same fiber cable.

Optical Modulation and Detection Technologies

Generally, there are three basic physical attributes of a light wave that can be modulated to carry information, its amplitude, phase, and polarization. As shown in Figure 4, there are three popular modulation and detection schemes, intensity modulation and direct detection (IM/DD), differential phase keying (DSPK), and coherent optical modulation and detection. For IM/DD, the most common optical modulation format is on-off-keying (OOK), in which the light intensity is turned on and off to represent the "1" and "0" states of a digital signal. OOK is widely used in early optical fiber communication systems because of its simple transmitter and receiver configuration, but its receiver sensitivity and spectral efficiency are quite limited as compared with most other modulation formats.

For DSPK, the commonly used formats are differential binary-phase-shift keying (DBPSK) and differential quadrature-phase-shift keying (DQPSK), which utilizes the phase difference between adjacent symbols to carry information bits. For DBPSK detection, an optical delay interferometer (ODI) is used to compare the signal with a delayed copy of itself and convert the phase modulation into intensity modulation that can be directly detected by square-law detectors. This detection scheme can be extended to DQPSK that carries 2 bits per symbol by using two ODIs with a 90-degree phase offset.

For coherent optical modulation, both the in-phase (I) and quadrature (Q) components of each of two orthogonal polarizations of an optical carrier can be modulated. For coherent optical detection, the coherent optical signal to be received mixes with a reference optical carrier that is provided by an optical local oscillator (OLO). Both polarization diversity and phase diversity are applied to allow for retrieving four orthogonal components of the received optical signal, I and Q components of two orthogonal polarization states. High-speed analog-to-digital converters (ADCs) are used to sample the four retrieved orthogonal components for follow-up digital signal processing (DSP) that recovers the original information bits carried by the coherent optical signal. This type of receiver is commonly referred to as digital coherent receiver (DCR), and the DSP used in recovering the optical signal is sometimes referred to as oDSP where "o" indicates the optical nature of the signal being processed. As the full electromagnetic field of the optical signal is reconstructed by the DCR, all the linear effects experienced by the optical signal during fiber

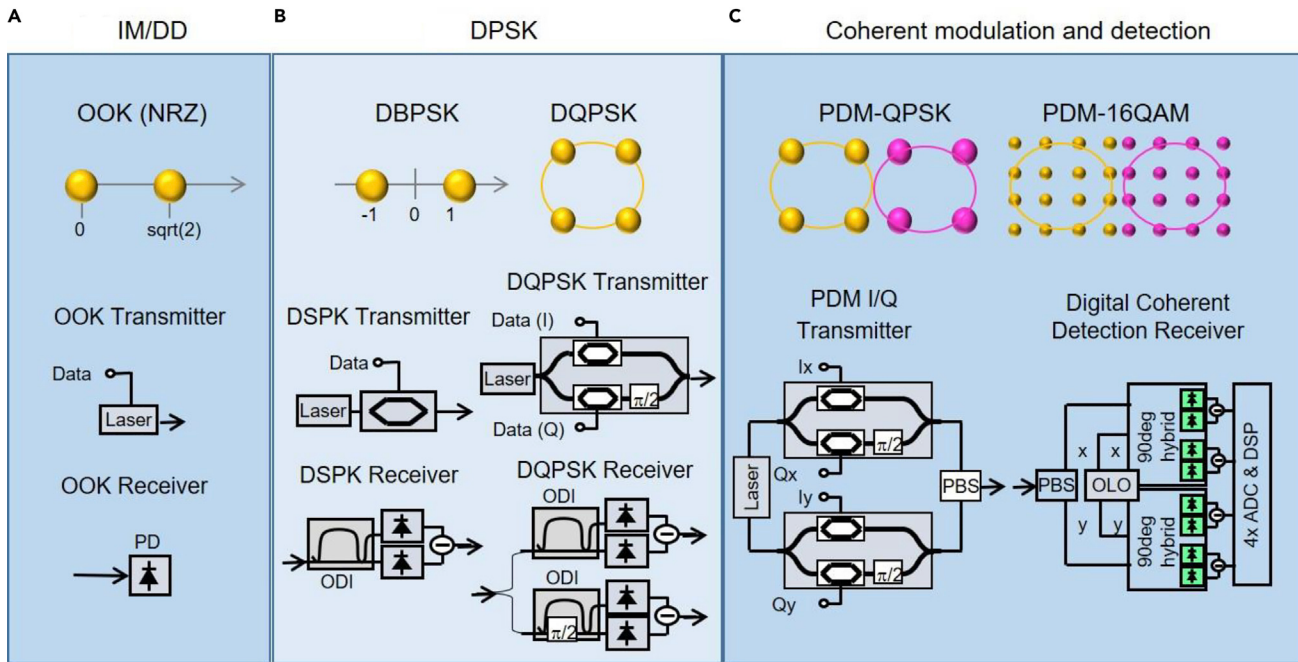


Figure 4. Illustration of Three Commonly Used Modulation and Detection Schemes

(A) Intensity-modulation and direct-detection (IM/DD), (B) differential phase-shift keying (DPSK), and (C) coherent optical modulation and digital coherent detection. PBS, polarization beam splitter; OLO, optical local oscillator; ADC, analog-to-digital converter; DSP, digital signal processing.

transmission, such as chromatic dispersion (CD), polarization rotation, and polarization-mode dispersion (PMD), can be fully compensated by using linear digital filters (Taylor, 2004; Noe, 2005; Ly-Gagnon et al., 2006; Leven et al., 2006; Savory, 2008; Sun et al., 2008). This is a very powerful technology that essentially enabled today's high-speed transmission at a per-wavelength data rate of 100 Gb/s and above.

With the access to the full optical field information at both transmitter and receiver, modern coherent optical communications have benefited from many powerful DSP techniques originally developed for wireless communication. However, data rates in optical communication are usually several orders of magnitude higher than those in wireless communication, necessitating efficient DSP techniques tailored specifically for optical communications, indeed reflecting a statement by Haykin (2001), "Signal processing is at its best when it successfully combines the unique ability of mathematics to generalize with both the insight and prior information gained from the underlying physics of the problem at hand." For optical communications in single-mode fiber, channel equalization can be efficiently realized by separating slowly varying transmission effects such as chromatic dispersion (CD) from rapidly varying effects such as polarization rotations and polarization-mode dispersion (PMD).

Figure 5 shows the block diagrams of common DSP modules implemented in a polarization-diversity DCR. First, compensation of chromatic dispersion is conducted by using a linear filter that is relatively static, as the chromatic dispersion of a given fiber link is virtually fixed. Second, clock recovery is performed to extract the signal modulation symbol rate. Third, PMD compensation and polarization demultiplexing are realized by a dynamic 2-by-2 linear filter, as polarization state of the received signal may vary very quickly owing to vibrations and temperature changes occurred along the fiber link. This dynamic filter is usually based on the constant-amplitude algorithm (CMA) for typical QPSK and nQAM modulation formats. Fourth, laser frequency offset estimation (FOE) is performed for each polarization component of the optical signal to digitally compensate for the frequency offset between the center frequency of the received signal and the OLO. Fifth, laser phase estimation (PE) is performed to align the phase between the optical carrier of the signal and the OLO so that the signal constellation can be recovered. The ability to digitally perform the FOE and PE allows the OLO to be free running, without the need for a sophisticated optical phase-locked loop (OPLL), thereby enabling the practical implementation of coherent detection. Sixth, demodulation is conducted to recover the information bits carried by the optical signal. Finally, forward-error

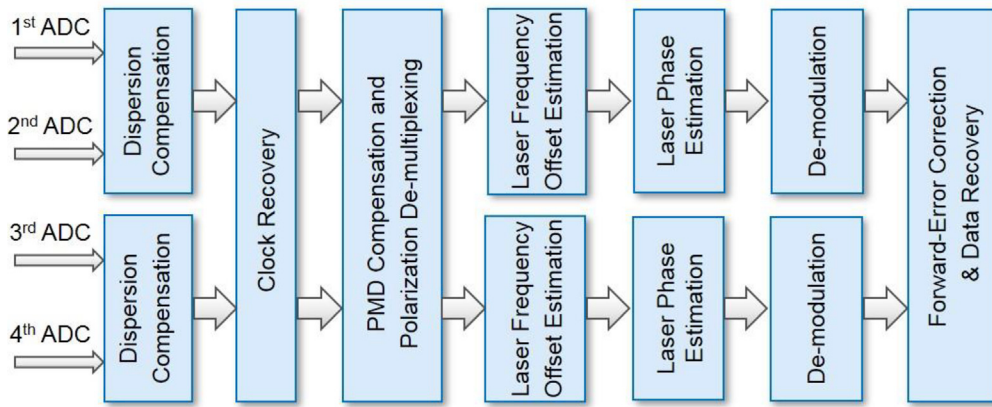


Figure 5. Block Diagram of Common DSP Modules Implemented in the DSP Unit of a Polarization-Diversity Digital Coherent Receiver

correction (FEC) is applied to increase the fidelity of the recovered information bits. As the digitally recovered signal constellation has a resolution of multiple bits in each quadrature, soft-decision (SD) FEC decoding can be applied to achieve better error-correction performance than previously used hard-decision (HD) FEC decoding, showing another major benefit of digital coherent detection.

Figure 6 illustrates the recent advances in per-fiber capacity from 8 Tb/s typically in 2013 to 32 Tb/s in 2019, representing a remarkable increase of about 1 dB per year. In 2013, digital coherent detection with SD-FEC was enabling 100-Gb/s PDM-QPSK wavelength channels to be transmitted over long distances, e.g., over 4,000 km. With the typical C-band transmission with EDFA having an amplification bandwidth of 4 THz, eighty 50-GHz-spaced wavelength channels could be transmitted by a single optical fiber link, leading to a per-fiber capacity of 8 Tb/s. The spectral efficiency (SE) of the WDM system was thus typically 2 b/s/Hz. The opto-electronic (OE) devices needed for modulation at the transmitter and detection at the receiver were typically specified at 32 Gbaud, as it allowed PDM-QPSK to provide a raw data rate of 128 Gb/s, sufficient to guarantee a net data rate of 100 Gb/s after removing overheads used for FEC etc. The oDSP was typically based on 40-nm CMOS technology.

In 2016, higher-level modulation such as PDM-16QAM was commercially deployed to double the per-channel data rate to 200 Gb/s, the WDM system SE to 4 b/s/Hz, and the per-fiber capacity to 16 Tb/s. To achieve longer transmission distance for 200-Gb/s channels, 64-Gbaud PDM-QPSK was commercialized, thanks to the availability of OE devices with doubled speed and the deployment of flexible-grid WDM in which the channel spacing can be flexibly adjusted at the increment of 12.5 GHz. A typical channel spacing for 200-Gb/s PDM-QPSK channels is 75 GHz, resulting in a WDM SE of 2.67 b/s/Hz. To allow the optical signal to be tolerant to bandwidth limitations due to cascaded optical filtering, faster-than-Nyquist (FTN) algorithm was developed. The oDSP for 200-Gb/s coherent receivers was typically based on 16-nm CMOS technology.

In 2019, even higher level QAM modulations such as PDM-64QAM was introduced to further increase the transmission system SE. Constellation shaping, particularly probabilistic constellation shaping (PCS), has been introduced to further improve coherent optical transceiver performance to better approach the Shannon capacity limit at high SE (Buchali et al., 2016; Cho et al., 2018; Lotz et al., 2013). Field trials on the use of real-time PCS-enabled coherent transceivers had also been demonstrated, achieving a 2-fold increase in reach when PCS is activated (Li et al., 2018). The 400-Gb/s wavelength channels were transmitted over a 75-GHz-spaced flexible-grid WDM system, leading to a further increased WDM SE of 5.3 b/s/Hz. The oDSP for 400-Gb/s coherent receivers was typically based on 7-nm CMOS technology. With an innovative design, the spectral bandwidth of the C-band of EDFA was broadened from its typical value of 4 THz by 50% to 6 THz, forming the so-called Super-C-band (Huawei's ON2.0, 2019). In the Super-C-band, eighty 75-GHz-spaced 400-Gb/s channels can be supported, thus achieving a further doubled per-fiber capacity of 32 Tb/s.

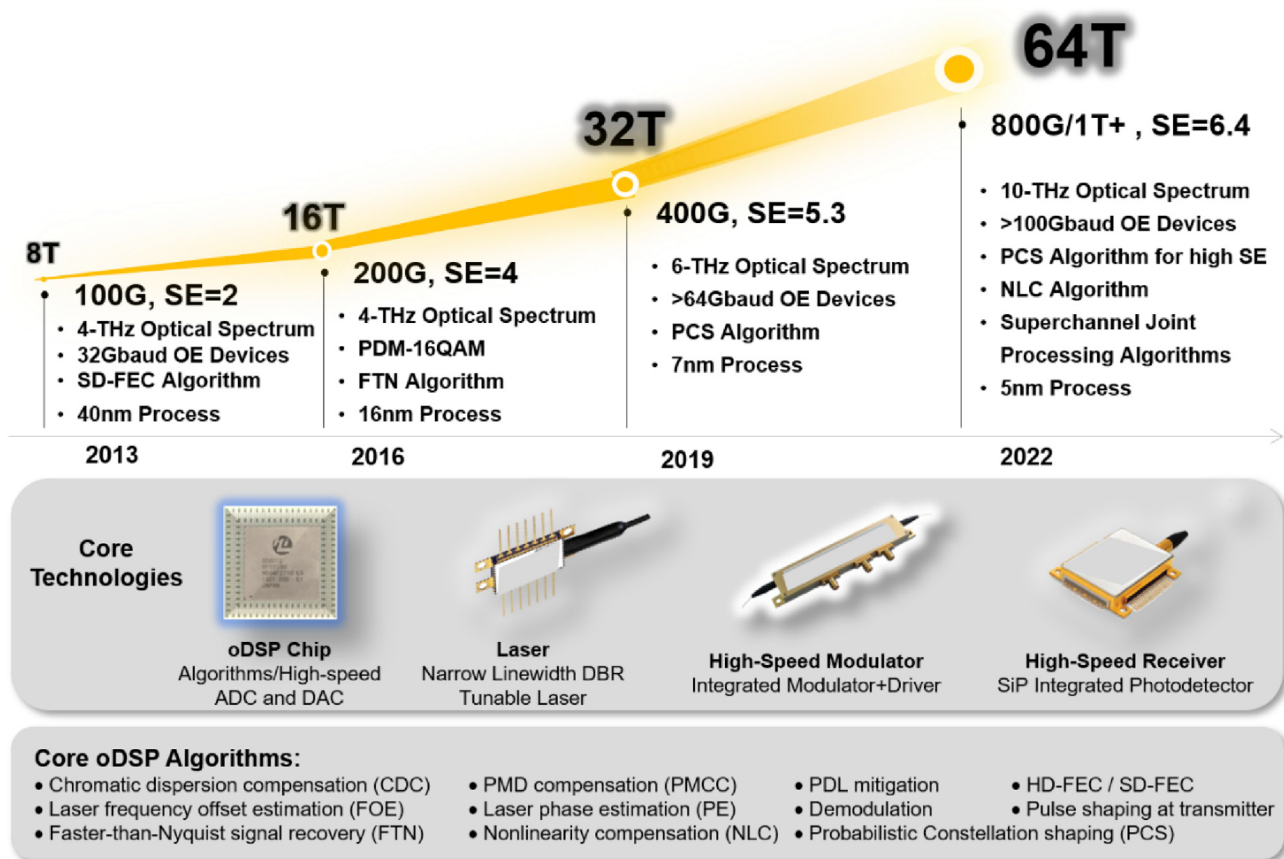


Figure 6. Illustration of Recent Advances in Per-fiber Capacity from 8 Tb/s Typically in 2013 to 32 Tb/s in 2019

Going forward, we expect further advances in broadening the amplification bandwidth of EDFA, increasing the OE device speeds and adopting more advanced oDSP algorithms, as shown in Figure 6. With the use of both the extended C-band and the extended L-band, the amplification bandwidth of EDFA may be increased to 10 THz and beyond. With advances in OE device technologies, the modulation speed may exceed 100 Gbaud. More advanced oDSP algorithms include PCS for higher-level QAM, nonlinearity compensation (NLC), and joint processing of superchannel constituents may be implemented with 5-nm CMOS technology. With the above-mentioned potential advances, further doubling of per-fiber capacity to 64 Tb/s may be achieved in commercial systems in 2022.

Superchannel Transmission

To further scale up the optical interface data rate beyond the bandwidth of OE devices, the concept of superchannel with optical parallelism was introduced. The first experimental demonstration of long-haul superchannel transmission, when the term “superchannel” was coined for this type of application, was performed by Bell Labs’ S. Chandrasekhar and X. Liu in 2009 (<https://en.wikipedia.org/wiki/SuperChannel>). Initially, the term superchannel referred to multiple single-carrier-modulated signals that are seamlessly multiplexed under the coherent optical orthogonal frequency-division multiplexing (CO-OFDM) conditions. The superchannel concept was later generalized to any collection of optical signals that are

- (1) modulated and multiplexed together with high SE at a common originating site,
- (2) transmitted and routed together over a common optical link, and
- (3) received at a common destination site.

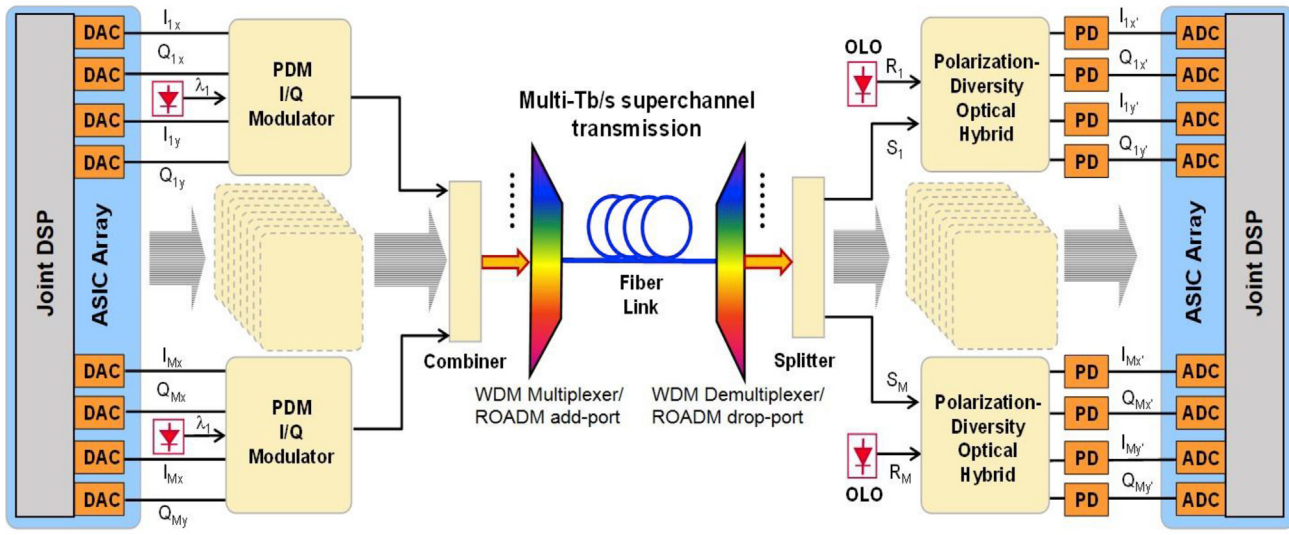


Figure 7. Illustration of a Superchannel Transponder Embedded in a Flexible-Grid WDM System

DSP, digital signal processor; DAC, digital-to-analog converter; ASIC, application-specific integrated circuit; PDM, polarization-division multiplexed; WDM MUX (DMUX), wavelength-division multiplexer (de-multiplexer); OLO, optical local oscillator; PD, photo-detector; ADC, analog-to-digital converter (after Ref. Liu et al., 2014).

There are a few comprehensive reviews on the superchannel technology (Liu et al., 2014; Chandrasekhar and Liu, 2019). To achieve high-SE multiplexing, "Nyquist-WDM" and "quasi-Nyquist-WDM" with spectrally shaped single-carrier modulated signals have also been introduced, offering an alternative to OFDM with trade-offs in spectral efficiency, DSP complexity, opto-electronic hardware complexity, and subcarrier access possibilities. From a networking point of view, the introduction of Tb/s-class superchannels has led to a rethinking of the spectral bandwidth allocation in optical fibers. Although most current systems operate on a rigid 50-GHz WDM channel grid, Tb/s-class superchannels benefit from so-called flexible grid WDM systems that allow for more efficient utilization of the optical spectrum (see, e.g., ITU-T G.694.1, "Spectral grids for WDM applications: DWDM frequency grid"). Figure 7 illustrates a multi-Tb/s superchannel transmitted over a flexible-grid WDM system.

The key benefits of superchannels in a flexible-grid WDM system are:

- (1) Higher spectral efficiency (SE) in WDM transmission, by reducing the percentage of wasted optical spectrum between individual channels,
- (2) Better leverage of large-scale photonic integrated circuits and application-specific integrated circuits (ASICs),
- (3) The ability to meet the demand of high-speed serial interface rates, which increases faster than the speed provided by opto-electronic converters (O/E), electro-optic converters (E/O), DACs, and ADCs,
- (4) The feasibility to perform joint processing of superchannel constituents to further improve transmission performance, and
- (5) Reduced number of optical-routing paths/ports in reconfigurable optical add/drop multiplexers (ROADMs), by aggregating more capacity in optically routed superchannels.

As the constituents of a superchannel share the same optical transmission path, they experience some common transmission properties. Hence, the monitoring of some transmission properties of the superchannel can be simplified by monitoring only one of the constituents, or more accurate measurements can be obtained by averaging certain channel estimates across superchannel constituents. For example, if the source lasers of the superchannel constituents are frequency locked, as in the case of CO-OFDM, the frequency estimation of a superchannel can be simplified. As the signal fields of all constituents are

available at the receiver, joint DSP can be applied to mitigate certain impairments, such as coherent cross talk between adjacent signals.

For DSP-efficient dispersion compensation of superchannels, sub-band equalizers and filter-bank based digital sub-banding have been proposed. In these approaches, a superchannel is divided into multiple sub-bands, which are individually dispersion-compensated to achieve higher DSP efficiency and easier parallelization. In addition, joint FEC using all the superchannel constituents may provide additional performance improvements.

Fiber nonlinearity is a major transmission impairment in optical fiber communications. In contrast to static nonlinearities encountered in some radio-frequency systems, fiber transmission suffers from the interplay of power-dependent phase distortions within and across WDM channels, coupled with chromatic dispersion that induces correlation across hundreds of symbols. Mathematically, fiber transmission in two polarizations is described by the coupled nonlinear Schrödinger equation (NLS). Digital backpropagation (DBP) as a means to numerically invert the NLS at the receiver (Li et al., 2008; Ip and Kahn, 2008) has been introduced to mitigate signal-to-signal nonlinear interactions such as self-phase modulation (SPM) and cross-phase modulation (XPM). With the availability of the signal fields of all the constituents of a superchannel, joint DBP can be applied to mitigate both SPM and XPM impairments (Liu et al., 2014), potentially making superchannel transmission performance better than independent transmission of its sub-channels.

Exploring the Capacity Limit in Optical Fiber Transmission

In information theory, there is a well-known Shannon-Hartley theorem that states that the maximum rate at which information can be transmitted over a communications channel (C) of a specified bandwidth (B) in the presence of noise is (Shannon, 1948)

$$C = B \log_2 \left(1 + \frac{S}{N} \right) \quad (\text{Equation 1})$$

where S is the average power of the received signal over the bandwidth and N is the average power of the noise over the bandwidth. S/N is the signal-to-noise ratio (SNR) at the receiver.

Assuming that the signal distortions due to fiber nonlinearity are Gaussian distributed, which is a reasonably accurate assumption for dispersion-uncompensated high-speed transmission links (Bosco et al., 2011; Poggolini et al., 2014), we can define an effective SNR as the ratio between the signal power and the sum of the linear noise resulting from ASE and the nonlinear noise (Chandrasekhar and Liu, 2019)

$$\text{SNR} = \frac{P}{\sigma_L^2 + \sigma_{NL}^2} = \frac{1}{aP^{-1} + bP^2} \quad (\text{Equation 2})$$

where P , δ_L^2 , and δ_{NL}^2 are, respectively, the signal power, linear noise power, and nonlinear noise power, and a and b are parameters that depend on link conditions. The SNR is maximized to

$$\text{SNR}_{\max} = a^{-2/3} b^{-1/3} / \left(2^{1/3} + 2^{-2/3} \right) \quad (\text{Equation 3})$$

at the optimum power $P_{opt} = \left(\frac{a}{2b} \right)^{1/3}$. Evidently, the SNR penalty due to fiber nonlinearity (as compared with the case without fiber nonlinearity) at the optimal signal launch power is $-10\log(2/3) \approx 1.76$ dB. This is in good agreement with that obtained through numerical simulations for dispersive coherent transmission (Bosco et al., 2011; Poggolini et al., 2014). We have the following key observations:

- (1) Reducing the linear (L) noise power coefficient a down by 3 dB causes P_{opt} to decrease by 1 dB and SNR_{\max} to increase by 2 dB;
- (2) Reducing the nonlinear (NL) noise power coefficient b down by 3 dB causes P_{opt} to increase by 1 dB and SNR_{\max} to increase by 1 dB;
- (3) At the optimal power P_{opt} , the linear and nonlinear noise powers are 2/3 and 1/3 of the total noise power, respectively.

Assuming that the transmission link consists of uniform fiber spans with the same physical characteristics and seamless multiplexing of signals with the same modulation format, the maximum effective SNR can be further expressed as (Chandrasekhar and Liu, 2019)

$$SNR_{\max} = \frac{(8\pi\alpha|\beta_2|)^{1/3}}{3[3n_0^2\gamma^2N_s h_e \ln(B/B_0)]^{1/3}} \quad (\text{Equation 4})$$

where α , β_2 , and γ are the fiber coefficients for loss, dispersion, and nonlinearity, respectively; N_s is the number of fiber spans of the optical link; n_0 is the power spectral density of the optical amplified spontaneous (ASE) noise, which is proportional to $N_s \cdot 10^{\alpha L_s}$ (where L_s is the length of each fiber span); B is the bandwidth of the WDM signals; B_0 is related to the CD-induced walk-off bandwidth; and h_e is the nonlinear multi-span noise enhancement factor. The maximum SNR is obtained at the optimum signal power spectral density

$$I_{\max} = \left(\frac{8n_0\pi\alpha|\beta_2|}{3\gamma^2N_s h_e \ln(B/B_0)} \right)^{1/3} \quad (\text{Equation 5})$$

For dispersion-uncompensated optical transmission (DUMT) or dispersion compensation module (DCM) free transmission, which is a popular approach enabled by the capability of electronic dispersion compensation in digital coherent receivers, $h_e \approx 1$, and we have

$$SNR_{\max,DUMT} \propto \frac{[\alpha|\beta_2|/\ln(B/B_0)]^{1/3}}{N_s 10^{2\alpha L_s/3}\gamma^{2/3}} \quad (\text{Equation 6})$$

and

$$I_{\max,DUMT} \propto 10^{\alpha L_s/3} [\alpha|\beta_2|/\ln(B/B_0)]^{1/3} \gamma^{-2/3} \quad (\text{Equation 7})$$

The maximum signal quality factor (Q^2) of a signal with nQAM modulation format has the following approximate dependence on link parameters:

$$Q_{\max,DUMT}^2 \propto \frac{SNR_{\max,DUMT}}{n} \propto \frac{[\alpha|\beta_2|/\ln(B/B_0)]^{1/3}}{n N_s 10^{2\alpha L_s/3}\gamma^{2/3}} \quad (\text{Equation 8})$$

The maximum achievable SE obtained by using PDM-nQAM for the link is achieved by setting the maximum signal quality factor equal to the quality factor corresponding to the underlying FEC threshold, Q_{FEC}^2 ,

$$SE_{\max,DUMT} = 2 \log_2(n) = 2 \log_2 \left(\frac{s[\alpha|\beta_2|/\ln(B/B_0)]^{1/3}}{N_s 10^{2\alpha L_s/3}\gamma^{2/3} Q_{FEC}^2} \right) \quad (\text{Equation 9})$$

where the first number 2 is for PDM and s is a scaling factor. By setting the maximum signal quality factor Q_{\max}^2 to the FEC threshold Q_{FEC}^2 , we can express the achievable transmission distance ($L_{\text{Achievable}}$) for a nQAM signal in given fiber link as

$$L_{\text{Achievable}} = N_s L_s = \frac{s(\alpha|\beta_2|)^{1/3} L_s}{n 10^{2\alpha L_s/3}\gamma^{2/3} Q_{FEC}^2} \quad (\text{Equation 10})$$

The above-mentioned analytical results suggest the following key transmission characteristics in DUMT:

- (1) To increase spectral efficiency by 2 bit/s/Hz, one could increase the dispersion coefficient ($|\beta_2|$) by a factor of 8, reduce the nonlinear coefficient (γ) by a factor of $2^{1.5}$ (or 2.83), reduce the loss per span by a factor of $\sim 2^{1.5}$, or reduce the number of fiber spans (N_s) by a factor of 2. These analytical findings are in reasonable agreement with those obtained through numerical simulation.
- (2) The optimum signal power spectral density is dependent on fiber parameters but is independent of the transmission distance and the modulation format (Bosco et al., 2011).
- (3) The optimum signal quality factor Q^2 scales inversely proportional to the transmission distance. The physical reason behind this is that, in DUMT, the nonlinear noises (or distortions) generated by the fiber spans are de-correlated, so the accumulation of the nonlinear noise during transmission scales the same way as the linear noise resulting from the ASE.

- (4) Reducing the FEC threshold (Q_{FEC}^2) by 3 dB leads to doubled transmission distance, showing the importance of using powerful FEC codes with higher coding gains, e.g., SD-FEC codes, to enable longer transmission distance.
- (5) For a given fiber link, the achievable transmission distance is inversely proportional to the constellation size (n). For example, if a PDM-QPSK signal can reach 4,000 km in a dispersion-unmanaged fiber link, then the transmission distances of PDM-16QAM and PDM-64QAM would be reduced to about 1,000 and 250 km, respectively. Note that, with PCS, the achievable transmission distance may be increased when the net SE is adjusted lower.

The above findings from the analytical study are in reasonably good agreement with the results obtained by experiments and numerical simulations for DUMT of superchannels based on O-OFDM and Nyquist-WDM ([Bosco et al., 2011](#)). The above analysis is based on several assumptions, such as homogeneous fiber spans, negligible signal-to-noise nonlinear interaction, and ideal transceivers having zero implementation penalty.

New optical fibers that provide lower loss coefficient (α), higher dispersion, and/or smaller nonlinear coefficient (γ), e.g., by increasing its effective area (A_{eff}), can increase SE and transmission distance. A useful method to compare the transmission performances of different fiber types is to use a figure of merit (FOM) for a given fiber that determines its transmission distance advantage (in dB) over a reference fiber, which is typically set to be the standard ITU G.652.D optical fiber. With the aforementioned analytical results, we can approximately define the FOM as

$$FOM = \frac{2}{3}(\alpha_{ref}L - \alpha L) + \frac{1}{3} \cdot 10 \log \left[\left(\frac{A_{eff}}{A_{eff, ref}} \right)^2 \left(\frac{L_{eff, ref}}{L_{eff}} \right) \left(\frac{D}{D_{ref}} \right) \right] \quad (\text{Equation 11})$$

For example, we can set the reference fiber as a G.652.D fiber that has the following parameters:

$$L = 100 \text{ km}, \alpha_{ref}L = 20 \text{ dB}, A_{eff, ref} = 85 \mu\text{m}^2, L_{eff, ref} = 21.5 \text{ km}, D_{ref} = 17 \text{ ps/nm/km}.$$

Recently, a new class of fiber suitable for long-haul transmission has been standardized by the ITU as G.654.E. This class of fibers are commercially available, such as OFS's TeraWave fiber and Corning's TXF™ fiber ([See, n.d.](#)). The new ITU G.654.E-compliant fiber typically has the following parameters ([See, n.d.; Shen et al., 2017](#)):

$$L = 100 \text{ km}, \alpha L = 17 \text{ dB}, A_{eff} = 125 \mu\text{m}^2, L_{eff} = 25 \text{ km}, D = 21 \text{ ps/nm/km}.$$

Based on [Equation 11](#), the FOM of the new G.654.E fiber is about 3 dB w.r.t. the reference fiber. This means that the new fiber may provide twice the reach as compared with the reference fiber. If the transmission distance is set to be the same as the reference fiber link, a 3-dB increase in FOM can be used to increase the SE by about 2 b/s/Hz, based on our previous analysis. A more rigorous definition of FOM with the consideration of splicing loss differences is provided by [Hasegawa et al. \(2017\)](#).

With the combined use of G.654.E-compliant fiber, C + L band EDFA, and advanced oDSP such as PCS, a single-fiber capacity of 100.5 Tb/s was recently demonstrated over a 600-km fiber link ([Yu et al., 2018](#)). More specifically, WDM transmission of 195 50-GHz-spaced channels with a net WDM SE of 10.3 b/s/Hz and a total EDFA amplification bandwidth of 9.75 THz was demonstrated, achieving a total single-fiber capacity of 100.5 Tb/s. The transmission fiber link consisted of six spans of 100-km G.654E-compliant fiber. [Figure 8](#) shows the measured optical spectrum of the 195 wavelength channels after 600-km optical fiber transmission. This demonstration shows the power of the combined use of better fiber, wider EDFA amplification bandwidth, and advanced oDSP for achieving high single-fiber capacity. It is worth noting that, in parallel to increasing single-fiber capacity, reducing cost-per-bit and energy-consumption-per-bit via device technologies such as silicon photonics and photonic integration is also of vital importance.

Reconfigurable Optical Add/Drop and Optical Cross-Connect

5G applications impose a stringent requirement on overall network latency. To effectively transport WDM channels with low latency, it is highly preferred to adopt optical wavelength switching as much as possible

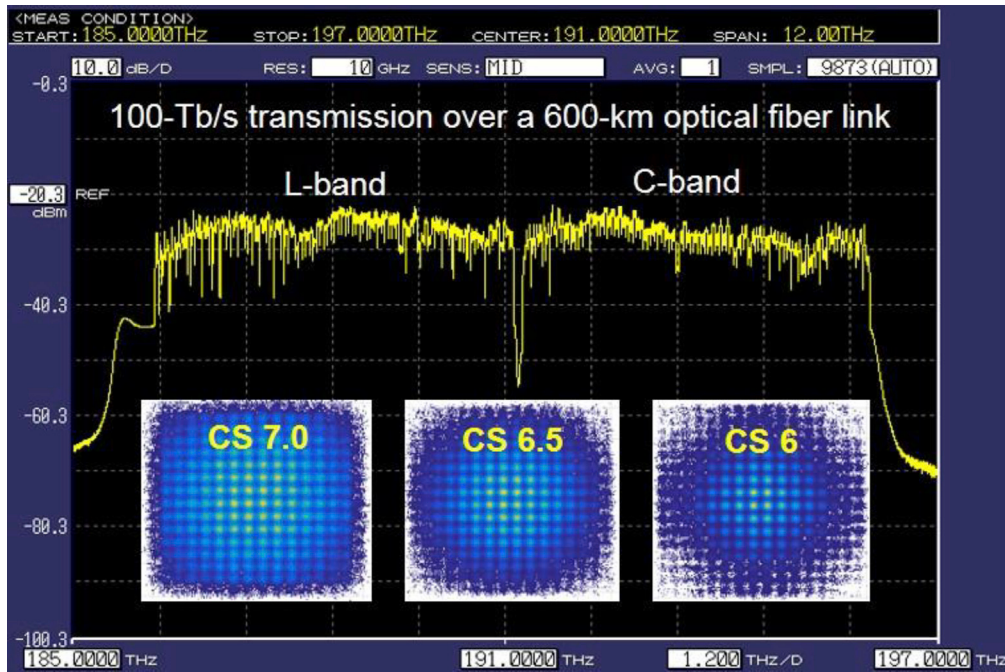


Figure 8. Experimental Demonstration of Single-Fiber Transmission with a Capacity of 100.5 Tb/s

Experimentally measured optical spectrum of 195 50-GHz-spaced wavelength channels with a net WDM SE of 10.3 b/s/Hz and a total EDFA amplification bandwidth of 9.75 THz, achieving a total single-fiber capacity of 100.5 Tb/s. Insets: constellation diagrams with different constellation shaping (CS) values.

to achieve direct wavelength pass-through at the optical layer (L0) over various nodes of the 5G-oriented optical networks. Thus, massive optical cross-connections are needed to provide the full switching capability for all the WDM channels in all the fibers connected to an optical node. The industry has evolved from the conventional OADM era to the multi-degree (MD) ROADM era. Currently, much effort has been devoted to enhancing the $1 \times N$ wavelength selective switch (WSS)-based MD-ROADM, by eliminating the number of inter-port fiber connections with an all-optical backplane and by using $N \times M$ WSS to improve reliability. Figure 9 illustrates a ROADM/OXC node supporting the adding/dropping of any wavelength to/drop from any direction. Traditional WSS based on multi-cast switches (MCSs) may be upgraded to a novel add/drop WSS (ADWSS) that replaces MCS with wavelength-selective components to achieve lowered loss and power consumption (Zong et al., 2016; Colbourne et al., 2018). Going forward, the ROADM/OXC subsystem may become even more compact by using an integrated $N \times N$ OXC at the wavelength level for line-side switching and an integrated $N \times M$ WSS for local add/drop and fiber-free connections.

Ultrabroadband Optical Access

Passive optical network (PON) is playing an important role in supporting broadband access to residential users, business customers, and 5G base stations, as shown in Figure 10. The 2.5-Gb/s GPON and EPON systems have been widely deployed around the world, and 10-Gb/s PON has started to be deployed. As the key next-generation optical access technology, 50-Gb/s passive optical network (50G-PON) is currently being standardized by ITU-T. For downstream transmission, the signal wavelength has been chosen to be $1,342 \pm 2$ nm. It was recently shown that the use of receiver-side equalization (EQ) (Liu and Effenberger, 2016; Houtsma and van Veen, 2017; Zeng et al., 2019) and advanced forward-error correction (FEC) can support 50-Gb/s downstream transmission over 20-km standard single-mode fiber (SSMF) at the 1342-nm wavelength with PR30 (29dB) link budget (Tao et al., 2019). For upstream transmission, the key signal data rate under consideration is 25 Gb/s, and the signal center wavelengths being considered include 1,300 and 1,270 nm. Recently, 25-Gb/s burst-mode upstream transmission by using a high-power and cost-effective 1270-nm directly modulated laser (DML) was demonstrated (Zeng et al., 2019). With a novel DSP-assisted burst-mode

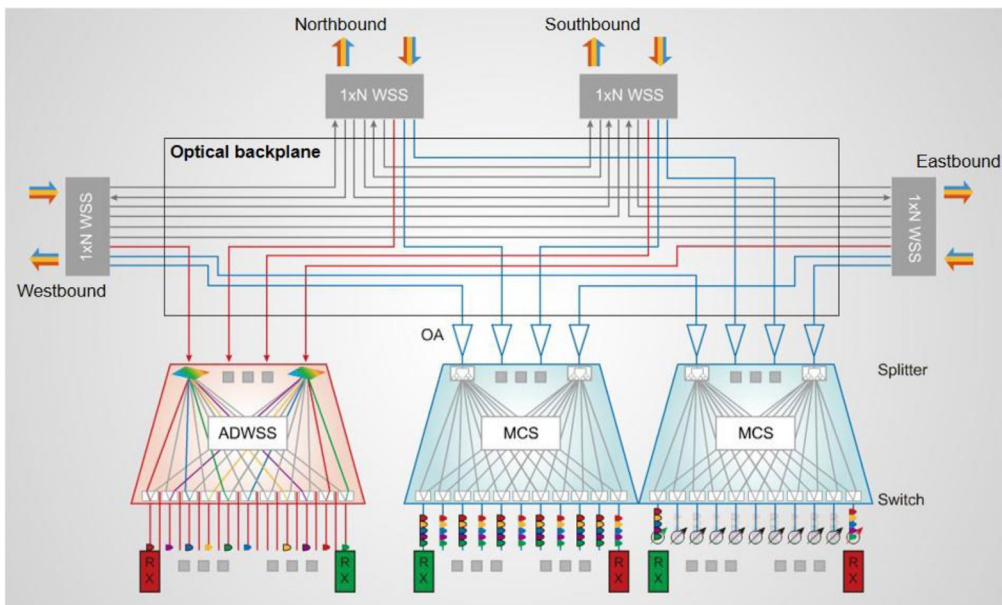


Figure 9. Illustration of a ROADM/OXC Node Supporting the Adding/Dropping of Any Wavelength to/Drop from Any Direction

MCS, multi-cast switches used in traditional WSS. ADWSS, a new type of add/drop WSS that replaces MCS with wavelength-selective components to offer lowered loss and power consumption. OA, Optical amplifier.

receiver, a record receiver sensitivity of -29.8 dBm was achieved at the SD-LDPC BER threshold of 2×10^{-2} after 20-km SSMF transmission, leading to a high link budget of over 34 dB. In addition, fast burst synchronization and recovery were realized within ~ 200 ns, even in the presence of multiple unequal-power bursts per PON frame, paving the way for supporting future low-latency access applications such as 5G fronthauling and virtual reality (VR).

5G-ORIENTED OPTICAL TRANSPORT NETWORK

Mobile network applications have a diverse set of demands such as ultra-low latency, ultra-high availability, ultra-large bandwidth, and overall optimization of the entire network. With the use of software-defined network (SDN), intelligent optical networks can be built with the network virtualization and slicing capabilities for 5G (Liu and Deng, n.d.). To more efficiently carry the upcoming 5G client signals, the “full-stack” OTN can be simplified as well as enhanced to focus on 5G services. Because of the well-defined time-division-multiplexing (TDM)-based multiplexing and switching in OTN, guaranteed low latency can be achieved to effectively meet the 5G networking latency requirement.

C-RAN is playing an important role in mobile networks by improving network performance via CoMP and increasing network energy efficiency via capacity sharing and optimization (Huang et al., 2014). Mobile fronthaul is a key network element in the C-RAN architecture, as it connects centralized baseband units (BBUs) with remote radio units (RRUs) (Pizzat et al., 2015). The interface for mobile fronthaul is primarily based on the common public radio interface (CPRI) (CPRI Specification V7, 2015) and the evolved CPRI (eCPRI) (The CPRI, 2017) via a point-to-point (PTP) architecture. Mobile front-haul could also be used to support massive multiple-input-multiple-output (M-MIMO), which is considered as another key technology for 5G networks. On the other hand, mobile back-haul connects BBUs with the core networks to transport the baseband data streams to their respective destinations.

In 5G, BBU and RRU may evolve into centralized unit (CU), distributed units (DU), and active antenna unit (AAU), and the transmission link is expected to be partitioned to three sections as follows (Liu and Deng, n.d.):

- (1) The front-haul section connecting AAUs and DUs;

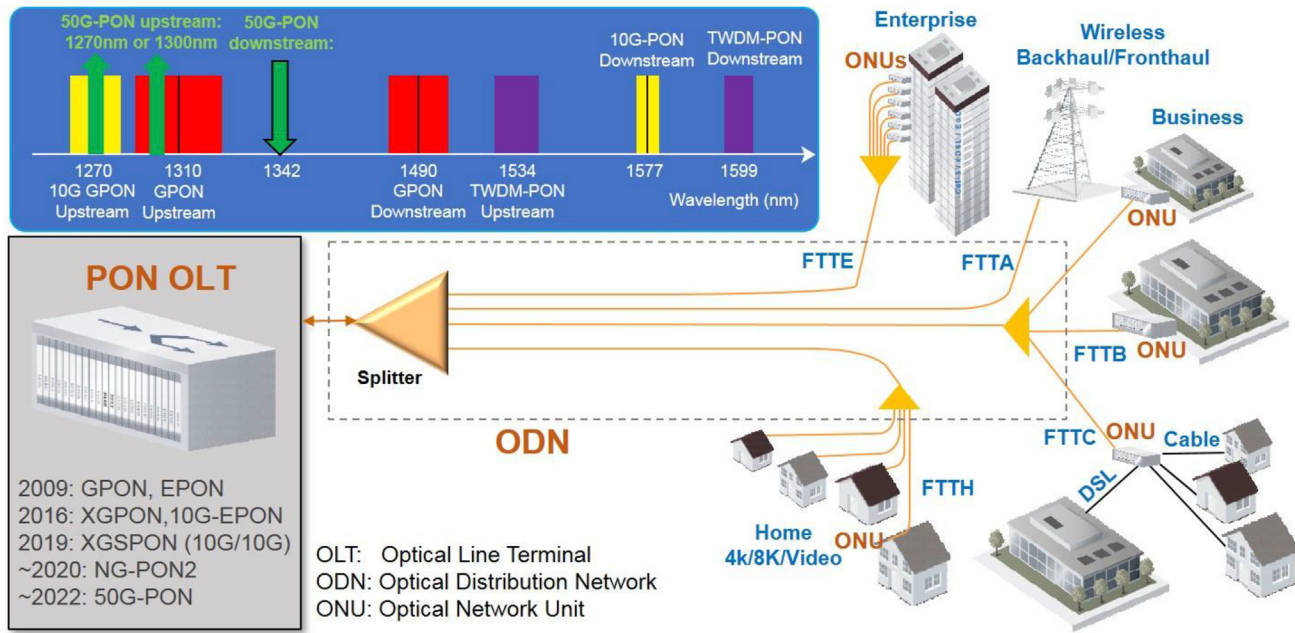


Figure 10. Illustration of Passive Optical Network (PON) Supporting Broadband Connectivity for Fiber-to-the-home (FTTH), Fiber-to-the-business (FTTB), Fiber-to-the-antenna (FTTA), Fiber-to-the-enterprise (FTTE), and Fiber-to-the-copper (FTTC) Applications

- (2) The mid-haul section connecting DUs and CUs; and
- (3) The back-haul section connecting CUs and the core network.

These three sections are generally referred to as X-haul sections. CPRI is the commonly used interface for mobile front-haul, connecting the radio frequency (RF) equipment with the physical layer (PHY) processing in radio equipment control (REC). To obtain a balanced trade-off between transmission throughput and processing complexity for a given application scenario, at radio equipment site, there are more functional split options available. A popular functional split for the front-haul section is defined by the CPRI industry association as the evolved (or Ethernet-based) CPRI, referred to as eCPRI, which connects the lower-level portion of the PHY layer with the higher-level portion of the PHY layer.

To support X-haul transmission, single-fiber bidirectional (BiDi) transmission with two wavelengths, passive WDM, WDM-PON, and active WDM are commonly used technologies (Liu and Deng, n.d.). Depending on the X-haul transmission scenario, a given technology may be chosen to satisfy the transmission requirements with minimal total cost of ownership (TCO).

Figure 11 shows one example of using mobile-optimized OTN equipment to support front-haul with high bandwidth efficiency, low cost, high reliability, accurate synchronization among the connected nodes, and iQ&M. To achieve high reliability, path protection can be applied. To achieve accurate synchronization among the connected nodes, precision time protocol as defined by the IEEE 1588 standard (Edison, 2006) can be applied. To maintain wireless services even in the event of path protection, latency compensation needs to be applied to ensure that the protection path and the original path are equal in propagation delay, as illustrated in Inset (a). To achieve iO&M, it is desirable for OTN to be able to sense the CPRI information and conduct configuration and negotiation automatically, as illustrated in Inset (b).

INTELLIGENT NETWORK OPERATION AND MAINTENANCE

Figure 12 illustrates an intelligently managed optical network with intelligent network operation and maintenance (iO&M). In the network deployment phase, iO&M enables fast network planning, service initiation, and provisioning. In the operation phase, traffic forecast, troubleshooting, and failure warning can be

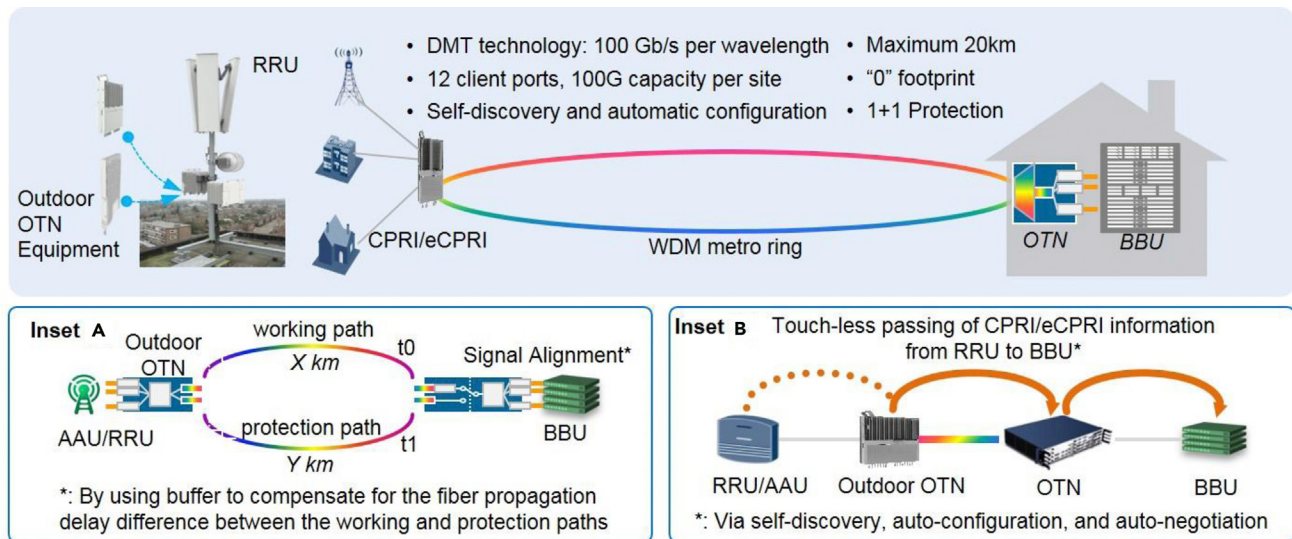


Figure 11. Illustration of a Mobile-Optimized Optical Transport Network (M-OTN) for Fronthaul

Inset (A): latency compensation between the original and protection paths. Inset (B): easy OAM via self-sensing of CPRI information and automatic negotiation and configuration.

supported. In the optimization phase, adaptive resource management and network slicing partition the network in such a way that a given service is adequately supported by a network slice in a resource-efficient manner (Vilalta et al., 2018). With the introduction of artificial intelligence (AI) in the network cloud engine (NCE), it is feasible to predict faults on optical networks and better anticipate future network resource requirements, thus improving O&M efficiency and marking a critical step toward zero-touch optical networks. To realize the above-mentioned iO&M features, the network controller needs to know the key parameters of the underlying physical layer of the optical network, as shown in Figure 12. These physical-layer

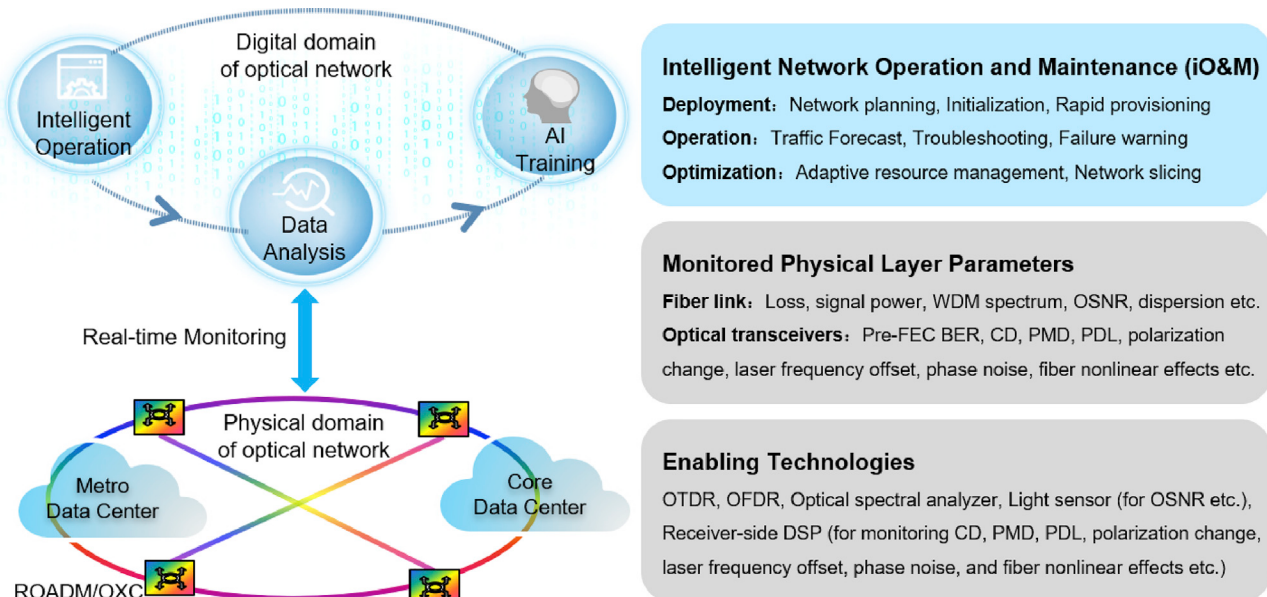


Figure 12. Illustration of an Intelligently Managed Optical Network with Intelligent Network Operation and Maintenance (iO&M)

WDM, wavelength-division multiplexing; OSNR, optical signal-to-noise ratio; FEC, forward-error correction; BER, bit-error rate; CD, chromatic dispersion; PMD, polarization-mode dispersion; PDL, polarization-dependent loss; OTDR, optical time-domain reflectometer; OFDR, optical frequency-domain reflectometer.

parameters are obtained from “light sensors” based on optical time-domain reflectometer (OTDR) and optical frequency-domain reflectometer (OFDR).

Conclusion and Outlook

In summary, we have reviewed recent advances in fiber-optic transmission and networking technologies covering coherent optical modulation and detection, superchannel transmission, new fibers that offer lowered loss and nonlinearity, super-C-band EDFA amplification, ROADM/OXC, ultrabroadband optical access, mobile-oriented optical transport network, and intelligent network operation and maintenance. These key optical technologies collectively support the main features of eFTC, mOXC, and iO&M for 5G-oriented optical networks. It is expected that future advances in fiber-optic transmission and networking technologies, enabled by close cooperation and collaboration in the global telecommunication community, will bring unprecedented communication experience for our society in the upcoming era of 5G (The 3rd Generation Partnership Project (3GPP), 2019; ITU-T Technical Report, 2018; ITU towards IMT for 2020 and beyond, 2019) during the decade of the 2020s.

ACKNOWLEDGMENTS

I wish to thank many of my current and past colleagues at Futurewei Technologies for collaboration. Among them are Frank Effenberger, Huaiyu Zeng, Sharief Megeed, Naresh Chand, Ning Cheng, Yuanqiu Luo, Andy Shen, and Linlin Li. I also would like to acknowledge the valuable discussion with many Huawei colleagues working in both optical and wireless departments. Among them are Guangxiang Fang, Ning Deng, Min Zhou, Yin Wang, Lei Zhou, Huafeng Lin, Minghui Tao, Shengping Li, Jiang Qi, Liang Song, and Xiao Sun.

The progresses in the field of fiber-optic transmission and networking implicitly represent the works of many researchers and engineers around the world. Some of their works are cited in this paper. Particularly, we would like to acknowledge valuable discussion with experts from British Telecom, China Mobile, China Telecom, China Unicom, Ericsson, ETRI, Finisar, Georgia Institute of Technology, Lumentum, Nokia, NTT, and Orange Labs.

REFERENCES

- Agrell, E., Karlsson, M., Chraplyvy, A.R., Richardson, D.J., Krumrich, P.M., Winzer, P.J., Roberts, K., Fischer, J.K., Savory, S.J., Eggleton, B.J., et al. (2016). Roadmap of optical communications. *J. Opt.* 18, 063002.
- Bosco, G., Curri, V., Carena, A., Poggolini, P., and Forghieri, F. (2011). On the performance of Nyquist-WDM terabit superchannels based on PM-BPSK, PM-QPSK, PM-8QAM or PM-16QAM subcarriers. *J. Lightwave Technol.* 29, 53–61.
- Buchali, F., Steiner, F., Böcherer, G., Schmalen, L., Schulte, P., and Idler, W. (2016). Rate adaptation and reach increase by probabilistically shaped 64-QAM: an experimental demonstration. *J. Lightwave Technol.* 34, 1599–1609.
- S. Chandrasekhar, X. Liu, B. Zhu, and D.W. Peckham, Transmission of a 1.2-Tb/s 24-carrier no-guard-interval coherent OFDM superchannel over 7200-km of ultra-large-area fiber, in Proc. European Conf. Optical Communication (ECOC) 2009, Sept., paper PD2.6.
- Chandrasekhar, S., and Liu, X. (2019). Advances in Tb/s superchannels, Chapter 3 of Optical Fiber Telecommunications VI, I.P. Kaminov, T. Li, and A. Willner, eds. (Elsevier), pp. 751–784.
- Cho, J., Chen, X., Chandrasekhar, S., Raybon, G., Dar, R., Schmalen, L., Burrows, E., Adamiecki, A., Corteselli, S., Pan, Y., et al. (2018). Trans-Atlantic field trial using high spectral efficiency probabilistically shaped 64-QAM and single-carrier real-time 250-Gb/s 16-QAM. *J. Lightwave Technol.* 36, 103–113.
- Chraplyvy, A.R., Gnauck, A.H., Tkach, R.W., and Derosier, R.M. (1993). 8 x 10 Gb/s transmission through 280 km of dispersion-managed fiber. *IEEE Photon. Technol. Lett.* 5, 1233–1235.
- P.D. Colbourne, S. McLaughlin, C. Murley, S. Gaudet and D. Burke. (2018). Contentionless Twin 8x24 WSS with Low Insertion Loss, 2018 Optical Fiber Communications Conference and Exposition (OFC), PDP Th4A.1.
- CPRI Specification V7. (2015). Common Public Radio Interface (CPRI): Interface Specification. http://cpri.info/downloads/CPRI_v_7_0_2015-10-09.pdf.
- Eidson, J.C. (2006). Measurement, Control and Communication Using IEEE 1588 (Springer).
- Essiambre, R.-J., Kramer, G., Winzer, P.J., Foschini, G.J., and Goebel, B. (2010). Capacity limits of optical fiber networks. *J. Lightwave Technol.* 28, 662–701.
- Giles, C.R., and Desurvire, E. (1991). Modeling erbium-doped fiber amplifiers. *J. Lightwave Technol.* 9, 271–283.
- Hasegawa, T., Yamamoto, Y., and Hirano, M. (2017). Optimal fiber design for large capacity long haul coherent transmission [Invited]. *Opt. Express* 25, 706–712.
- Haykin, S. (2001). Signal processing: where physics and mathematics meet. *IEEE Signal Process. Mag.* 18, 6–7.
- Hecht, J. (2004). City of light: the story of fiber optics. *Sloan Technol.* <https://www.amazon.com/City-Light-Story-Optics-Technology/dp/0195108183>.
- Ho, K.-P. (2005). Phase-modulated Optical Communication Systems (Springer).
- Houtsma, V., and van Veen, D. (2017). A study of options for high-speed TDM-PON beyond 10G. *J. Lightwave Technol.* 35, 1059–1066.
- Gnauck, A.H., Raybon, G., Chandrasekhar, S., Leuthold, J., Doerr, C., Stutz, L., Agarwal, A., Banerjee, S., Grosz, D., Hunsche, S., et al. (2002). 2.5 Tb/s (64x42.7 Gb/s) transmission over 40x100 km NZDSF using RZ-DPSK format and all-Raman-amplified spans, Optical Fiber Communication Conference (OFC), PDP FC2.
- See, e.g., press release Huawei’s ON2.0 Leads the Commercial Use of All-Optical Networks ... (tagitnews.com/en/article/36282), 2019.
- Huang, C.I.J., Duan, R., Cui, C., Jiang, J., and Li, L. (2014). Recent Progress on C-RAN Centralization and Cloudification. *IEEE* 2, 1030–1039.
- Ip, E., and Kahn, J.M. (2008). Compensation of dispersion and nonlinear impairments using digital backpropagation. *J. Lightwave Technol.* 26, 3416–3425.

- ITU towards IMT for 2020 and beyond (2019). <https://www.itu.int/en/ITU-R/study-groups/rsg5/rwp5d/imt-2020/Pages/default.aspx>.
- ITU-T Technical Report. (2018). Transport network support of IMT-2020/5G. <https://www.itu.int/pub/T-TUT-HOME-2018>.
- I. Kaminow, T. Li, and A.E. Willner, eds. (2013). Optical Fiber Telecommunications VI (Elsevier). <https://www.amazon.com/Optical-Fiber-Telecommunications-VI-Photronics/dp/0123969603>.
- Kao, K.C., and Hockham, G.A. (1966). Dielectric-fibre surface waveguides for optical frequencies. *Proc. IEEE* 113, 1151–1158.
- Leven, A., Kaneda, N., Klein, A., Koc, U.-V., and Chen, Y.-K. (2006). Real-time implementation of 4.4 Gbit/s QPSK intradyne receiver using field programmable gate array. *Electron. Lett.* 42, 1421–1422.
- Li, X., Chen, X., Goldfarb, G., Mateo, E., Kim, I., Yaman, F., and Li, G. (2008). Electronic post-compensation of WDM transmission impairments using coherent detection and digital signal processing. *Opt. Express* 16, 880–888.
- Li, J., Zhang, A., Zhang, C., Huo, X., Yang, Q., Wang, J., Wang, J., Qu, W., Wang, Y., Zhang, J., et al. (2018). Field Trial of Probabilistic-Shaping-Programmable Real-Time 200-Gb/s Coherent Transceivers in an Intelligent Core Optical Network, Asia Communications and Photonics Conference (ACP), PDP Su2C.1.
- X. Liu, Optical Communication Technologies for 5G Wireless, 2019 Optical Fiber Communication Conference (OFC 2019), Short Course SC444.
- X. Liu and N. Deng, Emerging optical communication technologies for 5G, Chapter 17 of Optical Fiber Telecommunications VII (Edited by A. Willner).n.d.
- Liu, X., and Effenberger, F. (2016). Emerging optical access network technologies for 5G wireless [Invited]. *J. Opt. Commun. Networking* 8, B70–B79.
- Liu, X., Wei, X., Slusher, R.E., and McKinstry, C.J. (2002). Improving transmission performance in differential phase-shift-keyed systems by use of lumped nonlinear phase-shift compensation. *Opt. Lett.* 27, 1616–1618.
- Liu, X., Chandrasekhar, S., and Winzer, P.J. (2014). Digital signal processing techniques enabling multi-Tb/s superchannel transmission: an overview of recent advances in DSP-enabled superchannels. *IEEE Signal. Process. Mag.* 31, 16–24.
- Lotz, T.H., Liu, X., Chandrasekhar, S., Winzer, P.J., Haunstein, H., Randel, S., Corteselli, S., Zhu, B., Peckham, D.W., et al. (2013). Coded PDM-OFDM transmission with shaped 256-iterative-polar-modulation achieving 11.15-b/s/Hz intrachannel spectral efficiency and 800-km reach. *J. Lightwave Technol.* 31, 538–545.
- Ly-Gagnon, D.-S., Tsukamoto, S., Katoh, K., and Kikuchi, K. (2006). Coherent detection of optical quadrature phase shift keying signals with carrier phase estimation. *J. Lightwave Technol.* 24, 12–21.
- Mears, R.J., Reekie, L., Jauncey, I.M., and Payne, D.N. (1987). Low-noise Erbium-doped fiber amplifier at 1.54μm. *Electron. Lett.* 23, 1026–1028.
- Noe, R. (2005). PLL-free synchronous QPSK polarization multiplex/diversity receiver concept with digital I&Q baseband processing. *IEEE Photon. Technol. Lett.* 17, 887–889.
- Pizzinat, A., Chanclou, P., Saliou, F., and Diallo, T. (2015). Things you should know about fronthaul. *J. Lightwave Technol.* 33, 1077–1083.
- Poggiolini, P., Bosco, G., Carena, A., Curri, V., Jiang, Y., and Forghieri, F. (2014). The GN model of fiber non-linear propagation and its applications. *J. Lightwave Technol.* 32, 694–721.
- Recommendation ITU-T G.694.1. (2012). <https://www.itu.int/rec/T-REC-G.694.1>.
- Savory, S. (2008). Digital filters for coherent optical receivers. *Opt. Express* 16, 804.
- Schawlow, A., and Townes, C. (1958). Infrared and optical masers. *Phys. Rev.* 112, 1940–1949.
- See, for example, <https://fiber-optic-catalog.ofsoptics.com/Asset/TeraWave-Fiber-161-web.pdf>; and https://www.corning.com/media/worldwide/coc/documents/Fiber/WP8105_1.17.pdf.n.d.
- Shannon, C.E. (1948). A mathematical theory of communication. *Bell Syst. Tech. J.* 27, 379–423.
- S. Shen, G. Wang, H. Wang, Y. He, S. Wang, C. Zhang, C. Zhao, J. Li, and H. Chen. (2017). G.654.E Fibre Deployment in Terrestrial Transport System, in Optical Fiber Communication Conference (OFC), paper M3G.4.
- Sun, H., Wu, K.-T., and Roberts, K. (2008). Real-time measurements of a 40 Gb/s coherent system. *Opt. Express* 16, 873–879.
- M. Tao, J. Zheng, X. Dong, K. Zhang, L. Zhou, H. Zeng, Y. Luo, S. Li, and X. Liu, Improved Dispersion Tolerance for 50G-PON Downstream Transmission via Receiver-Side Equalization, OFC 2019, paper M2B.3.
- Taylor, M.G. (2004). Coherent detection method using DSP for demodulation of signal and subsequent equalization of propagation impairments. *IEEE Photon. Technol. Lett.* 16, 674–676.
- The 3rd Generation Partnership Project (3GPP) (2019). <http://www.3gpp.org/>.
- The CPRI. (2017). Specification eCPRI 1.0, Common Public Radio Interface: eCPRI Interface Specification.
- R. Vilalta, A.M. López-de-Lerma, R. Muñoz, R. Martínez, and R. (2018). Casellas, Optical Networks Virtualization and Slicing in the 5G era, Proc. OFC, M2A.4, San Diego, USA.
- Winzer, P.J. (2011). Energy-efficient optical transport capacity scaling through spatial multiplexing. *IEEE Photon. Technol. Lett.* 23, 851–853.
- Winzer, P.J., and Essiambre, R.-J. (2006). Advanced optical modulation formats. *Proc. IEEE* 94, 952–985.
- Winzer, P.J., Neilson, D.T., and Chraplyvy, A.R. (2018). Fiber-optic transmission and networking: the previous 20 and the next 20 years [Invited]. *Opt. Express* 26, 24190–24239.
- Xu, C., Liu, X., and Wei, X. (2004). Differential phase-shift keying for high spectral efficiency optical transmissions. *IEEE J. Selected Top. Quant. Electron.* 10, 281–293.
- Yu, Y., Jin, L., Xiao, Z., Yu, F., Lu, Y., Liu, L., Wu, W., and Li, L. (2018). 100.5Tb/s MLC-CS-256QAM Transmission over 600-km Single Mode Fiber with C+L Band EDFA, Asia Communications and Photonics Conference (ACP) (PDP Su2C.3).
- Zeng, H., Liu, X., Megeed, S., Shen, A., and Effenberger, F. (2019). Digital signal processing for high-speed fiber-wireless convergence [Invited]. *J. Opt. Commun. Networking* 11, A11–A19.
- H. Zeng, A. Shen, N. Cheng, N. Chand, F. Effenberger, and X. Liu (2019). High-Performance 50G-PON Burst-Mode Upstream Transmission at 25 Gb/s with DSP-Assisted Fast Burst Synchronization and Recovery, ACP 2019, paper T1G.3.
- Zhou, Y., Smith, K., West, S., Johnston, M., Weatherhead, J., Weir, P., Hammond, J., Lord, A., Chen, J., Pan, W., et al. (2016). Field Trial Demonstration of Real-Time Optical Superchannel Transport up to 5.6Tb/s over 359km and 2Tb/s over a Live 727km Flexible Grid Link using 64GBaud Software Configurable Transponders, OFC'16, PDP C-1.
- L. Zong, H. Zhao, Z. Feng, and Y. Yan (2016). Low-cost, Degree-expandable and Contention-free ROADM Architecture Based on M × N WSS, Optical Fiber Communication Conference (OFC), paper M3E.3.